Journal of
*Sensor and Actuator Networks*

MDPI

*Article*

# Interdigitated Gear-Shaped Screen-Printed Electrode Using G-PANI Ink for Sensitive Electrochemical Detection of Dopamine

**Pritu Parna Sarkar [1], Ridma Tabassum [2], Ahmed Hasnain Jalal [3], Ali Ashraf [4] and Nazmul Islam [3,*]**

[1] Department of Mechanical Engineering, The University of Texas Rio Grande Valley, Edinburg, TX 78539, USA; prituparna.sarkar01@utrgv.edu
[2] Department of Bioengineering, The University of Kansas, Lawrence, KS 66045, USA; ridma.tabassum@ku.edu
[3] Department of Electrical & Computer Engineering, The University of Texas Rio Grande Valley, Edinburg, TX 78539, USA; ahmed.jalal@utrgv.edu
[4] Department of Mechanical Engineering, The University of South Florida, Tampa, FL 33620, USA; aliashraf@usf.edu
* Correspondence: nazmul.islam@utrgv.edu

**Abstract:** In this research, a novel interdigitated gear-shaped, graphene-based electrochemical biosensor was developed for the detection of dopamine (DA). The sensor's innovative design improves the active surface area by 94.52% and 57% compared to commercially available Metrohm DropSens 110 screen-printed sensors and printed circular sensors, respectively. The screen-printed electrode was fabricated using laser processing and modified with graphene polyaniline conductive ink (G-PANI) to enhance its electrochemical properties. Fourier Transform Infrared (FTIR) Spectroscopy and X-ray diffraction (XRD) were employed to characterize the physiochemical properties of the sensor. Dopamine, a neurotransmitter crucial for several body functions, was detected within a linear range of 0.1–100 µM, with a Limit of Detection (LOD) of 0.043 µM (coefficient of determination, $R^2$ = 0.98) in phosphate-buffer saline (PBS) with ferri/ferrocyanide as the redox probe. The performance of the sensor was evaluated using cyclic voltammetry (CV) and Chronoamperometry, demonstrating high sensitivity and selectivity. The interdigitated gear-shaped design exhibited excellent repeatability, with a relative standard deviation (RSD) of 1.2% ($n$ = 4) and reproducibility, with an RSD of 2.3% ($n$ = 4). In addition to detecting dopamine in human serum, the sensor effectively distinguished dopamine in a ternary mixture containing uric acid (UA) and ascorbic acid (AA). Overall, this novel sensor design offers a reliable, disposable, and cost-effective solution for dopamine detection, with potential applications in medical diagnostics and neurological research.

**Keywords:** printable sensor design; flexible sensor applications; sensor coatings; dopamine



**Citation:** Sarkar, P.P.; Tabassum, R.; Jalal, A.H.; Ashraf, A.; Islam, N. Interdigitated Gear-Shaped Screen-Printed Electrode Using G-PANI Ink for Sensitive Electrochemical Detection of Dopamine. *J. Sens. Actuator Netw.* **2024**, *13*, 84. https://doi.org/10.3390/jsan13060084

Academic Editor: Lei Shu

Received: 29 October 2024
Revised: 1 December 2024
Accepted: 3 December 2024
Published: 6 December 2024



## 1. Introduction

Dopamine (DA), also known as 3-hydroxytyramine, is a vital catecholamine neurotransmitter in the central nervous system of mammals, playing a significant role in both the central nervous and cardiovascular systems [1]. Often referred to as the "feel-good" or "happy hormone", dopamine is associated with various vital functions, including motor control, hormone production, cognition, learning, and reward [2]. In healthy individuals, the concentration of dopamine in the blood is extremely low, ranging from 0 to 0.25 nM, while in urine, it ranges from 0.3 to 3.13 µM [3]. Abnormal levels of dopamine, whether too high or too low, can lead to various neurological disorders, including Parkinson's disease, elevated blood pressure, epilepsy, increased heart rate, schizophrenia, arrhythmia, and Alzheimer's diseases [4–6]. Also, it is considered one of the most common stress biomarkers in bodily fluids [3]. Therefore, it is essential to detect dopamine in bodily fluids using a selective, sensitive, simple, and cost-effective method. The detection of dopamine is particularly challenging with conventional electrodes due to its low concentrations in

bodily fluids and the presence of ascorbic acid (AA) and uric acid (UA), which can be easily oxidized at similar potentials to dopamine [6].

Electrochemical immunosensing has emerged as a promising label-free detection technology due to its high sensitivity, ease of fabrication and use, cost-effectiveness, and ability to selectively respond even in complex environments [7–10]. This method operates on the principle of detecting changes in the electrical properties of a conductive substrate when an analyte binds to a surface functionalized with specific antibodies. The observed electrical changes result from variations in the concentration of electroactive redox species at the electrode [11,12]. For the electrodes of electrochemical sensors, various conductive polymers [13,14] carbon and metal nanomaterials [15,16], and paper with conductive coatings [6,15] can be used. Commercial polymer films can be used to produce and pattern porous graphene films known as laser-induced graphene (LIG), which exhibit high electrical conductivity and can be easily patterned into electrodes [16]. Thus, LIG has attracted considerable interest and has been extensively studied in the field of electroanalytical chemistry for biochemical sensing and device fabrication. The performance of these LIG sensors can be improved by modifying the working electrode with various conductive polymers like poly(3,4-ethylenedioxythiophene) (PEDOT) [17], polypyrrole (PPy) [18], and polyaniline (PANI) [19,20] etc. Among them, PANI is a common π-electron conjugated conductive polymer widely employed in sensing, energy storage, anti-corrosion, and adsorption applications. It also offers advantages such as excellent electrical conductivity, environmental stability, chemical durability, ease of synthesis, and low cost [21,22].

Minta et al. [23] utilized PANI for the electrochemical detection of dopamine in a linear range between 0.8 and 20 μM, achieving an LOD of 430 nM. Ghosh et al. [24] modified a screen-printed electrode sensor using graphene polyaniline (G-PANI) ink to detect dopamine within the linear range of 1–5 μM in human serum. Baytemir et al. [25] and Mahalakshmi et al. [26] also used PANI for the detection of dopamine. These methods showed promising results, but their linear range does not fall in the biological range, using complex processes to fabricate, and are not cost-effective.

With this motivation, in this research, we have developed a novel, graphene-based electrochemical biosensor that is easy to fabricate, utilizing a simple one-step process that does not require a clean room setup. For the first time in the literature, this type of design was introduced, which increases the surface area by 94.52% compared to commercially available Metrohm DropSens 110 screen-printed sensors. The sensor integrates graphene conductive ink-polyaniline (G-PANI) with a laser-induced graphene (LIG) electrode to form the LIG/G-PANI sensor. The performance of this novel sensor has been evaluated using cyclic voltammetry (CV) and Chronoamperometry. The sensor demonstrates successful detection within a linear range of 0.1–100 μM, which exceeds the performance of most sensors discussed in the literature. The LOD using CV is 0.095 μM, and for Chronoamperometry, it is 0.043 μM in a buffer solution. In addition to its impressive LOD, the sensor exhibits excellent repeatability and strong reproducibility. Furthermore, the sensor is capable of detecting dopamine in human serum and can selectively differentiate dopamine from a ternary mixture of dopamine, uric acid, and ascorbic acid.

## 2. Related Work

The performance analysis of various electrochemical sensors for dopamine detection, including the one presented in this work, is summarized in Table 1. In comparison to the other sensors discussed here, our proposed sensor provides a broader linear range and a lower LOD, offering notable improvements in dopamine detection capabilities.

The table highlights the fact that most of the electrodes discussed here require lengthy and complex preparation processes. For example, Yang et al. fabricated an alkali-activated graphitized carbon (a-GC) electrode using fish scales as precursors via enzymolysis, activation and the two-step pyrolytic carbonization method, with $K_3[Fe(CN)_6]$ as the catalyst. Similarly, Zhang et al. used a multi-component modification process involving 3D flake nickel oxide/cobalt oxide with porous carbon nanosheets, carbon nanotubes, and elec-

trochemically reduced graphene oxide composites to enhance a glassy carbon electrode, resulting in a costly and time-intensive method. Additionally, most sensors have a linear detection range starting at 1 µM, which is insufficient for the biological range starting at 0.3 µM. In contrast, our study used an easy-to-fabricate graphene sensor that took nearly one minute to achieve a screen-printed sensor and detected dopamine from 0.1 µM to 100 µM, covering the full biological range. This was made possible by the novel interdigitated electrode design introduced in our paper, which offers a larger active surface area for ligand attachment—a unique approach not previously reported in the literature.

**Table 1.** Comparison of dopamine detection performance for different biosensors.

| Electrode | Technique | Linear Range (µM) | Limit of Detection (LOD) | Reference |
|---|---|---|---|---|
| Pretreated bare cardboard-screen-printed electrodes (PBC-SPEs) | Differential Pulse Voltammetry (DPV) | 5–1000 | 1.25 µM | [27] |
| PVA-ZnO. Modified screen-printed electrodes | Cyclic voltammetry (CV) | 100–600 | 0.1208 mM | [28] |
| Au-CNFs. Modified screen-printed electrodes | Cyclic voltammetry (CV), Differential Pulse Voltammetry (DPV), and Chronoamperometry (CA) | 2–16 | 0.4 µM | [29] |
| Alkali-activated graphitized carbon (a-GC). Modified screen-printed carbon electrode (a-GC/SPCE) | Differential Pulse Voltammetry (DPV) | 1–1000 | 0.25 µM | [30] |
| $CeO_2$:$BaMoO_4$ nanocomposite-based 3D-printed electrode | Cyclic voltammetry (CV) | 5–1000 | 4.52 µM | [31] |
| $Ti_3C_2$ Nano Layer-Modified Screen-Printed Electrode | Cyclic voltammetry (CV) | 0.5–600 | 0.15 µM | [32] |
| β-cyclodextrin/Ni-MOF/glassy carbon electrode | Differential Pulse Voltammetry (DPV) | 0.7–310.2 | 0.227 µM | [33] |
| NiO/CoO@PCNs/CNTs/erGO/GCE | DPV | 0.1–22.0 | 0.045 µM | [34] |
| Modified designed LIG/G-PANI | CV | 0.1–100 | 0.095 µM | Current research |
| Modified designed LIG/G-PANI | Chronoamperometry (CA) | 0.1–100 | 0.043 µM | Current research |

## 3. Materials and Methods

### *3.1. Materials*

Dopamine hydrochloride (CAS No: 62-31-7), Kapton polyimide film (HN type, 0.152 mm thickness), graphene nanoflakes (specific surface area: 20 to 40 $m^2/g$, conductivity: 8000 S/m), phytic acid (CAS No: 83-86-3), polyaniline (CAS Number: 62-53-3), silver ink, potassium hexacyanoferrate (III) (CAS No: 13746-66-2), potassium hexacyanoferrate (II) trihydrate (CAS No: 14459-95-1), Phosphate-Buffer Solution(10X, pH = 7.4), and human serum (H3667) were attained from Sigma Aldrich, St. Louis, MO, USA. The uric acid, 99% (CAS No: 69-93-2) and L-(+)-ascorbic acid, ACS, 99+% (CAS no: 50-81-7) were purchased from Thermo Fisher Scientific Chemicals Inc., Wyman Street, Waltham, MA, USA. The polydimethylsiloxane (PDMS) was prepared by mixing the SYLGARDTM 184 Silicone Elastomer Base with the SYLGARDTM 184 Silicone Elastomer Curing Agent in a ratio of 10:1. The commercial sensors were obtained from Metrohm Dropsens, Riverview, FL, USA, with dimensions of 3.38 cm × 1.02 cm × 0.05 cm. The working electrode (WE) had a diameter of 4 mm, with

both the WE and the counter electrode (CE) made of carbon, while the reference electrode (RE) was composed of silver.

### 3.2. Apparatus and Software

The three-electrode system was designed using AutoCAD software version: 24.2 named Autodesk Inventor (2023). LIG sensors were fabricated using a Glowforge Pro ($CO_2$ Laser, 45 watts) from Glowforge, Seattle, WA, USA. All electrochemical experiments were carried out with an Autolab Potentiostat PGSTAT302N from Metrohm, Riverview, FL, USA. The software used for PGSTAT302N is Nova 2.1. We obtained the FTIR data with a Thermo Scientific Nicolet iS5 FTIR Spectrometer (Thermo Scientific, Waltham, MA, USA). For the XRD analysis, we utilized the RIGAKU MiniFlex600 XRD machine (Rigaku Americas Corporation, Woodlands, TX, USA). The Zeiss field emission scanning electron microscope from Zeiss, Oberkochen, Germany, was employed to extract Scanning electron microscopy (SEM) images. For a uniform graphene polyaniline ink solution, a Hauschild SpeedMixer (Farmington Hills, MI, USA, SMART DAC 250-2000) was utilized. All the graphs were plotted using Origin Pro (Origin Lab Corporation, Northampton, MA, USA).

### 3.3. Synthesis of Graphene–Polyaniline Ink

To produce G-PANI ink, 1 g of graphene nanoflakes (GNF), 2 mL of polyaniline, 4 mL of phytic acid, and 6 mL of deionized (DI) water were combined using a planetary mixture (Figure 1e). To create an acidic environment for the enhancement of the electrical conductivity of PANI, phytic acid was used.

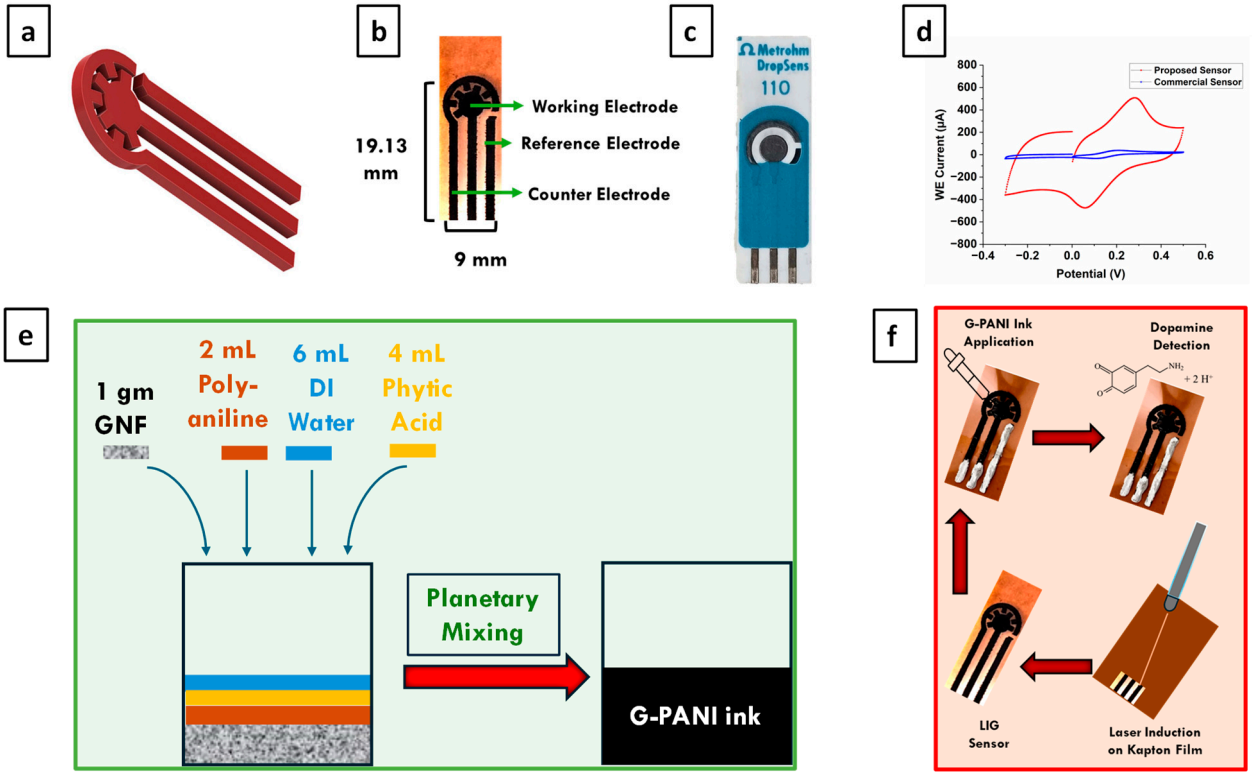


**Figure 1.** (**a**) CAD design of the interdigitated gear-shaped model, (**b**) in-house fabricated LIG sensor, and (**c**) commercially available sensor. (**d**) Comparison between the commercially available sensor with the proposed sensor. (**e**) Synthesis of G-PANI ink and (**f**) LIG sensor preparation.

### 3.4. Fabrication of the Electrode

A biosensor with dimensions of 19.13 mm in length, 9 mm in width, and a WE diameter of 5 mm was designed using Autodesk Inventor Figure 1a. This experiment employed a three-electrode system, as presented in Figure 1b, consisting of a reference

electrode (RE), working electrode (WE), and counter electrode (CE). The RE serves as a standard for measuring and regulating the WE potential, but it does not pass any current. The CE conducts all the current needed to balance the current at the WE. The design aimed to combine a conventional three-electrode system with an interdigitated electrode system to improve the active surface area of the biosensor, which would eventually provide more active sites for dopamine binding, thereby increasing the likelihood of detecting the biomolecule at significantly lower concentrations. The effective surface area was calculated using a quasi-Randles–Sevcik equation [35].

$$I^{quasi} = 0.436\, nFA_{real}C\sqrt{\frac{nFDv}{RT}}$$

Here, $n$ is the number of electrons that appeared in the half reaction for the redox pair, $v$ is the scan rate (V/s), $F$ is the Faraday's constant (96,485 C/mol), $A_{real}$ stands for the electroactive area of the electrode ($cm^2$), $R$ is the gas constant (8.314 J $mol^{-1}$ $K^{-1}$), $T$ is the absolute temperature (K), and $D$ is the diffusion coefficient of dopamine ($6.74 \times 10^{-6}$ $cm^2/s$). The effective area of the commercial sensor (shown in Figure 1c) was calculated to be 0.2028 $cm^2$, while the novel interdigitated gear-shaped electrode had an effective area of 3.7044 $cm^2$, successfully increasing the effective surface area by 94.52% (Figure 1d). Compared with the printed circular one, it showed an increase in the surface area of 57%.

We used the direct laser writing process on Kapton film using a 3D laser printer Glowforge Pro at a speed of 800× (i.e., 113 mm/s) and a precision power setting of 70% of the full 45-watt power for the fabrication of laser-induced graphene. In total, 70% isopropyl alcohol (IPA) was used for the initial wiping of the film. After manufacturing, we used our synthesized G-Pani ink to modify the WE (Figure 1f). The justification behind using G-Pani ink for the further modification of WE is briefly described in our previous paper [24]. After that, silver ink was manually applied to the contact pad of CE and WE as well as to create the reference electrode. The hydrophobic PDMS coating was then applied between the working zone and the contact pads to avert the analyte from flowing from the working zone to the contact pads. Once the sensor was fully prepared, it was left to dry overnight at room temperature (~25 °C).

### *3.5. Solution Preparation of Dopamine, Uric Acid and Ascorbic Acid*

First, 10× PBS was diluted with deionized (DI) water to prepare 1× PBS. Dopamine hydrochloride was then mixed with 1× PBS to prepare a dopamine stock solution. A range of dopamine concentrations from 0.01 µM to 100 µM was prepared using the serial dilution method. For the selectivity test, dopamine hydrochloride, uric acid, and ascorbic acid were mixed with the 1× PBS solvent.

### *3.6. Electrochemical Analysis of Dopamine*

The screen-printed electrode was connected to the Autolab Potentiostat using a three-electrode system cable connector. The potentiostat can handle a maximum current range of 2A and is integrated with Nova 2.1 software for electrochemical measurements. For the performance analysis of the novel interdigitated gear-shaped electrode, cyclic voltammetry (CV) and Chronoamperometry were conducted. The parameters for CV were set from −0.3 V to 0.5 V with a scan rate of 8 mV/s. For both CV and Chronoamperometry analysis, 10 µL of each concentration was applied to the WE, followed by a 10 min waiting period. After 10 min, another 10 µL of the same concentration, 10 µL of Ferrate ($Fe^{2+}$), and 10 µL of the Ferric ($Fe^{3+}$) solution (both prepared using 1× PBS solvent) were added, and the experiment was run. After each concentration test, the sensor was washed with 1× PBS and DI water before testing the next concentration.

## 4. Results and Discussion

### 4.1. Characterization

The intrinsic nanostructure and morphology of LIG combined with G-PANI ink, as well as the ink itself, were examined using scanning electron microscopy (SEM). The cross-sectional SEM image of the LIG/G-PANI ink revealed three distinct layers: the intact Kapton film layer, a middle layer of laser-induced graphene, and a porous layer of graphene–polyaniline ink (Figure 2a). From Figure 2b, a very porous top layer of the G-PANI ink is observed. It indicates a large surface area which can interact with the biomolecules.

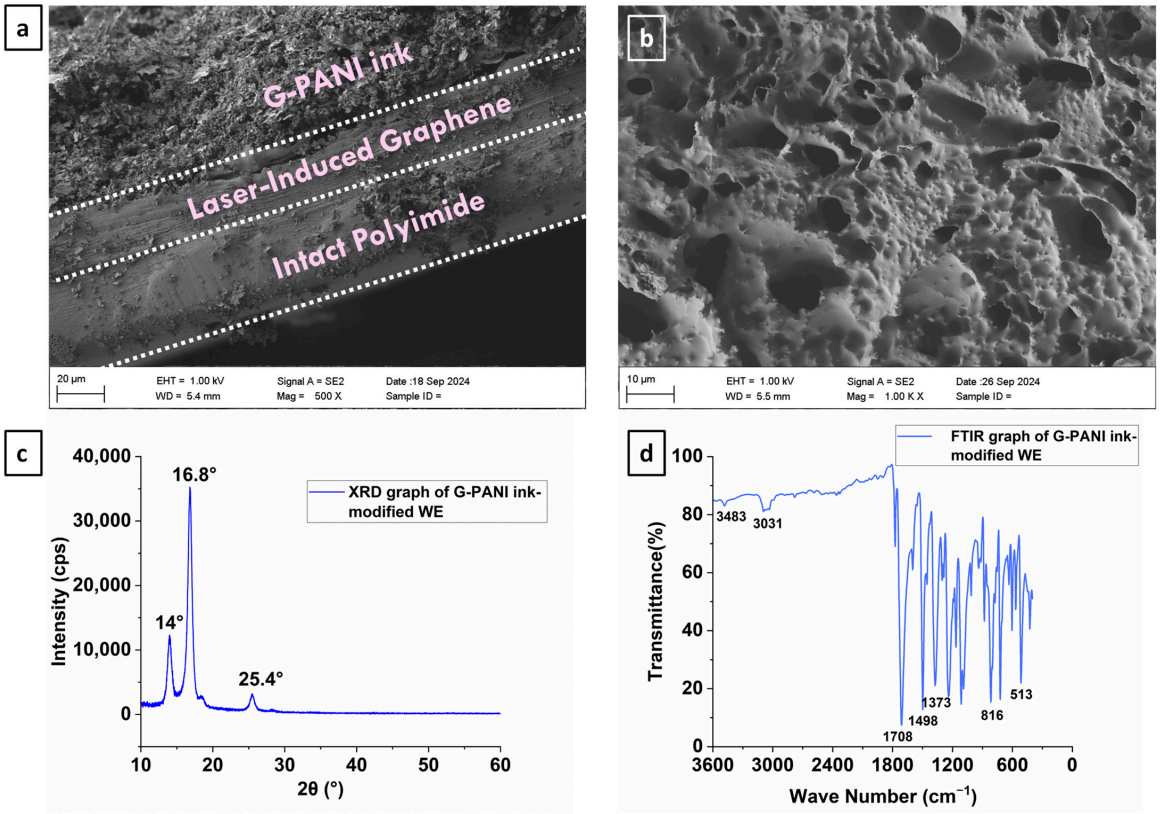


**Figure 2.** (**a**) Cross-sectional view of the G-PANI ink-coated LIG sensor. (**b**) The porous top view of G-PANI ink. (**c**) X-ray diffraction (XRD) spectra of the LIG/G-PANI ink showing the crystal structure of the ink. (**d**) Fourier Transform Infrared Spectroscopy (FTIR) spectroscopy of the LIG/G-PANI sensor.

The structural morphology of the designed LIG/G-PANI sensor analyzed by X-ray diffraction (XRD) shown in Figure 2c features a peak centered at 25.4°, corresponding to the (0 0 2) plane. The interlayer spacing ($I_c$) was calculated to be 3.5 Å using the equation $n\lambda = 2d\sin\theta$, indicating a high degree of graphitization in the LIG sensor [36].

Figure 2d of Fourier Transform Infrared Spectroscopy (FTIR) provides comprehensive details on the chemical bonds found in G-PANI conductive ink. N-H stretching vibrations, which are commonly linked to amine groups, are represented by the band at 3480 $cm^{-1}$ [37]. A prominent peak at 1708 $cm^{-1}$ indicates N = Q = N stretching, likely due to quinonoid structures in polyaniline. The peaks at 1498 $cm^{-1}$ and 1373 $cm^{-1}$ belong to C=C stretching and C-N bond stretching within the benzene ring of polyaniline [38]. The peaks at 815–516 $cm^{-1}$ are due to the bending of the aromatic C-H bond [39]. These peaks validate the successful synthesis and inclusion of polyaniline (PANI) in graphene-based ink.

### 4.2. Determination of Dopamine and Analytical Merits

In this study, the performance of the proposed novel interdigitated gear-shaped laser-induced Kapton sensor was evaluated by detecting dopamine. Both cyclic voltammetry (CV) and Chronoamperometry were used in the evaluation. CV was employed due to its

effectiveness as a widely used electrochemical technique for investigating the reduction and oxidation processes of molecular species [40]. Chronoamperometry, on the other hand, was employed to measure the current–time dependence for diffusion-controlled processes at an electrode, which varies with analyte concentrations [41].

The oxidation peak of the dopamine quasi-reversible redox couple typically occurs within the range of 0.1–0.3 V at a pH of approximately 7.4, particularly when graphene-based working electrodes are used [42]. As illustrated in Figure 3a, cyclic voltammograms (CVs) for dopamine concentrations ranging from 0.1 µM to 100 µM were analyzed using 1M PBS at a pH of 7.4 and a constant scan rate of 8 mV/s. Analyzing the curves for various dopamine concentrations, as presented in Figure 3a, a tendency is displayed for a declining WE oxidation current as the concentration rises. The linear regression equation I (µA) = −56.23 + 605.09 logC [dopamine concentration] and the coefficient of determination, $R^2$ = 0.94, explicitly demonstrate a linear relationship between the peak currents and the concentrations (Figure 3b). It is plausible that at very high concentrations, the diffusion of dopamine to the electrode surface became limited, leading to a lower effective concentration of dopamine at the electrode surface and, consequently, a lower current, even though the electrode surface was cleaned after each concentration [43]. The LOD was also calculated to be approximately 0.095 µM using the formula LOD = σ/S (where σ is the standard deviation of the response and S is the slope = 0.13 × slope of the semi-log plot) [44].

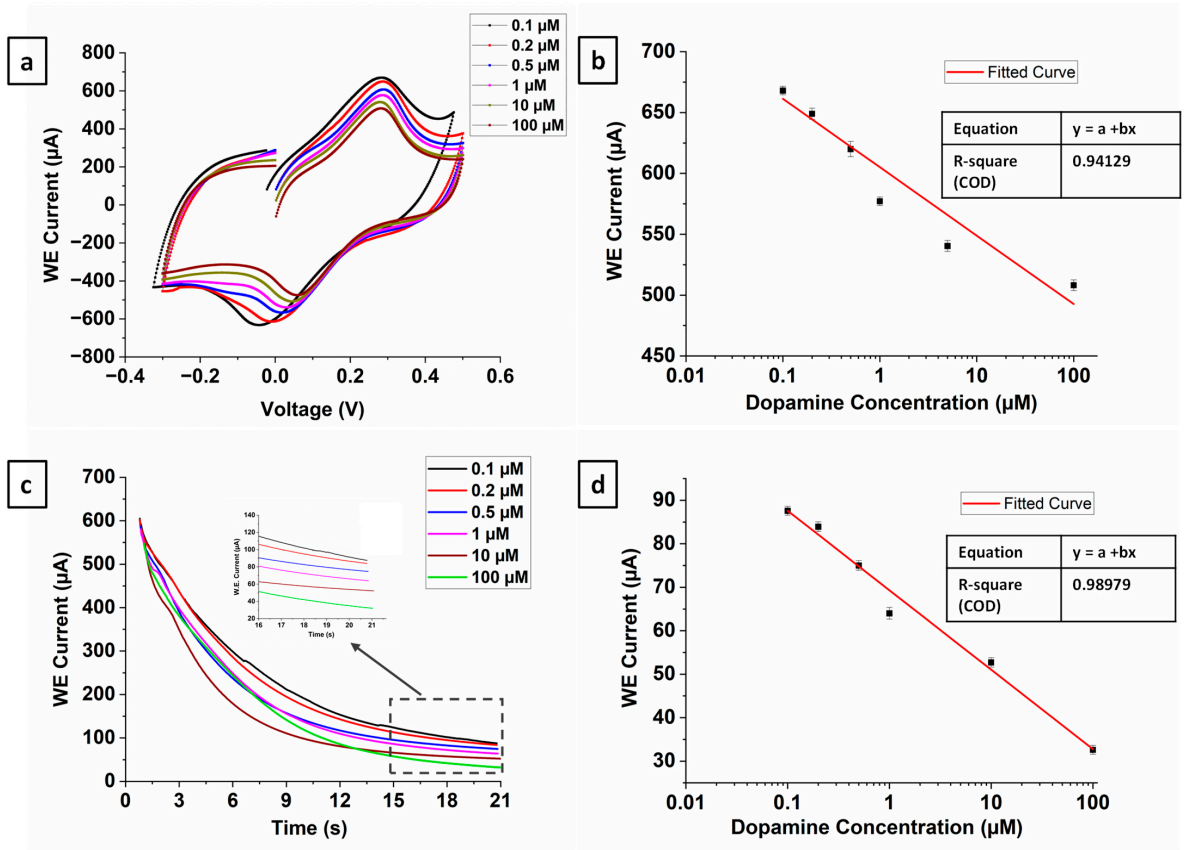


**Figure 3.** (**a**) CV curve of different concentrations of dopamine on interdigitated gear-shaped LIG/G-PANI sensor in 1M PBS (pH 7.4); (**b**) Linear relationship between peak current and concentration of dopamine; (**c**) Chronoamperometry curve of different concentrations of dopamine on interdigitated gear-shaped LIG/G-PANI sensor in 1M PBS (pH 7.4); (**d**) Linear relationship between stable WE current and concentration of dopamine.

Chronoamperometric measurements of dopamine at the LIG Kapton sensor were performed with the WE potential set at 0.3 V for both the first and second potential steps. The Chronoamperometric studies of dopamine solutions in PBS for ranges of concentrations

(0.1 µM–100 µM) are presented in Figure 3c. During the 20 s Chronoamperometric procedure, it was noted that the electrode's current rapidly dropped during the first 10 s, followed by rapid stabilization. The current decreased with the increasing dopamine concentration, following a similar trend of CV graphs. A possible reason for the decreasing current could be the polymerization of dopamine into polydopamine, which can coat the electrode surface, reducing the electroactive area and blocking electron transfer, particularly at higher concentrations. The interdigitated electrode design, with its closely spaced fingers, could also lead to increased resistance as the dopamine concentration rises, impeding efficient conductivity. These factors together contribute to the current drop. Figure 3d demonstrates a good linear response between the WE current and time. The coefficient of determination was found to be $R^2 = 0.98$, with the regression equation being I (µA) = −18.28 + 69.32 logC. The LOD was determined to be 0.043 µM.

### 4.3. Detection of Dopamine in Human Serum

Figure 4a illustrates that the novel interdigitated biosensor exhibits an almost linear trend for dopamine detection in human serum, comparable to the result of PBS. A lower current was seen for all serum concentrations, most likely because of the complex character of the serum, which influences the electron transfer process and restricts the amount of dopamine available for the interaction at the electrode surface. The calibration curve shown in Figure 4b for CV measurements in the serum is described by the regression equation, I (µA) = −38.5 + 293.2 logC, with a correlation coefficient of 0.958. Each concentration for dopamine was repeated four times to assess precision. This indicates that the sensor can successfully detect dopamine in human serum.

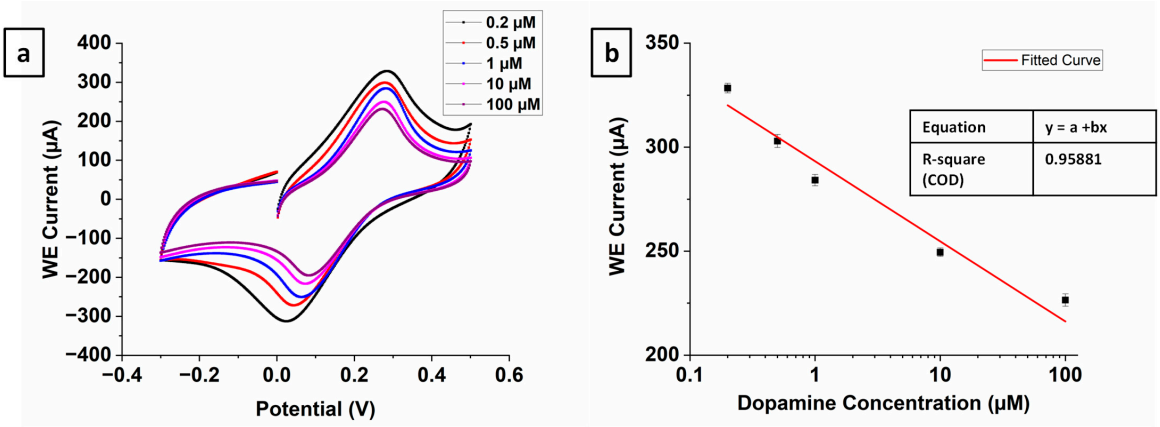


**Figure 4.** (**a**) CV curve of different concentrations of dopamine on interdigitated gear-shaped LIG/G-PANI sensor in human serum (**b**). A linear relationship between peak current and concentration of dopamine.

### 4.4. Selectivity of the Sensor

Selectivity refers to the ability of a bioreceptor to identify a specific analyte in a sample that contains various admixtures and contaminants, making it one of the most critical features of a biosensor [45]. For sensors designed to detect dopamine, selectivity is particularly important, as dopamine, ascorbic acid, and uric acid coexist in human serum as well as other extracellular body fluids. Most importantly, these three molecules tend to oxidize at nearly the same potential [46].

Figure 5a depicts the CV curve obtained using a ternary mixture of 0.5 mM dopamine (DA), 1 mM ascorbic acid (AA), and 0.8 mM uric acid (UA) in a 1M PBS solution at an 8 mV/s scan rate. As anticipated, the oxidation peak potentials of these three compounds are extremely near to one another and are distinctly observed at 0.28 V, −0.043 V, and 0.41 V, respectively. The peak potential separation (ΔE) between dopamine and AA is 0.33 V, dopamine and UA is 0.13 V, and UA and AA is 0.45 V. The bar graph (Figure 5b) makes it clear that there was no discernible change in the dopamine current level when a mixture of AA and UA was present. These noticeable variations in the anodic peak potentials

of dopamine, AA, and UA imply that the designed interdigitated gear-shaped biosensor measures dopamine selectively when the other two elements are present.

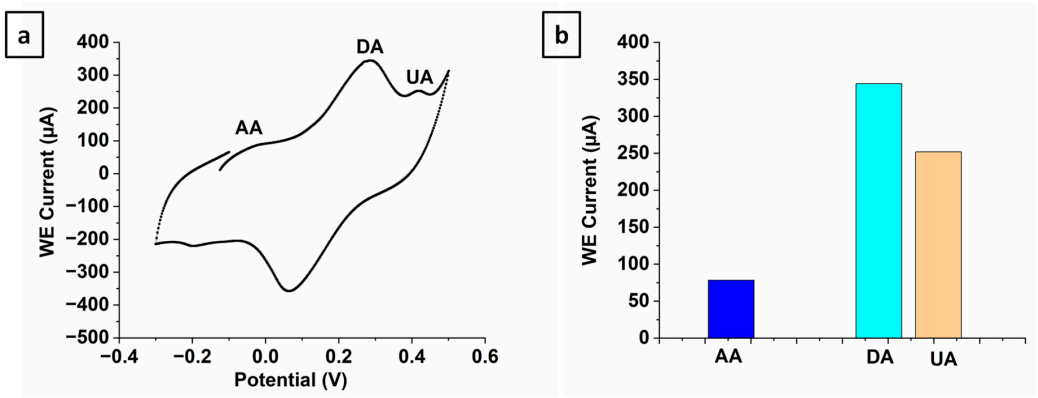


**Figure 5.** (**a**) CV curves measured for interdigitated gear-shaped LIG/G-PANI sensor using 0.1 M phosphate-buffer solution of pH 7.4 containing 1 mM ascorbic acid (AA), 0.5 mM dopamine (DA), and 0.8 mM uric acid (UA) (**b**) Bar graph corresponding to peak current of AA, UA, and dopamine.

### *4.5. Evaluation of Repeatability and Reproducibility of the Sensor*

To evaluate the repeatability of the biosensor, 200 nM of dopamine in 0.1 M PBS (pH 7.4) with $Fe^{2+}/Fe^{3+}$ redox couples was applied to the sensor. Four cyclic voltammograms were recorded successively at a scan rate of 8 mV/s using the same biosensor (Figure 6a). The histograms for repeatability shown in Figure 6b show that almost the same peak working electron current was observed for each measurement. The relative standard deviation (RSD) was calculated to be 1.2%, demonstrating that the sensor exhibits good repeatability.

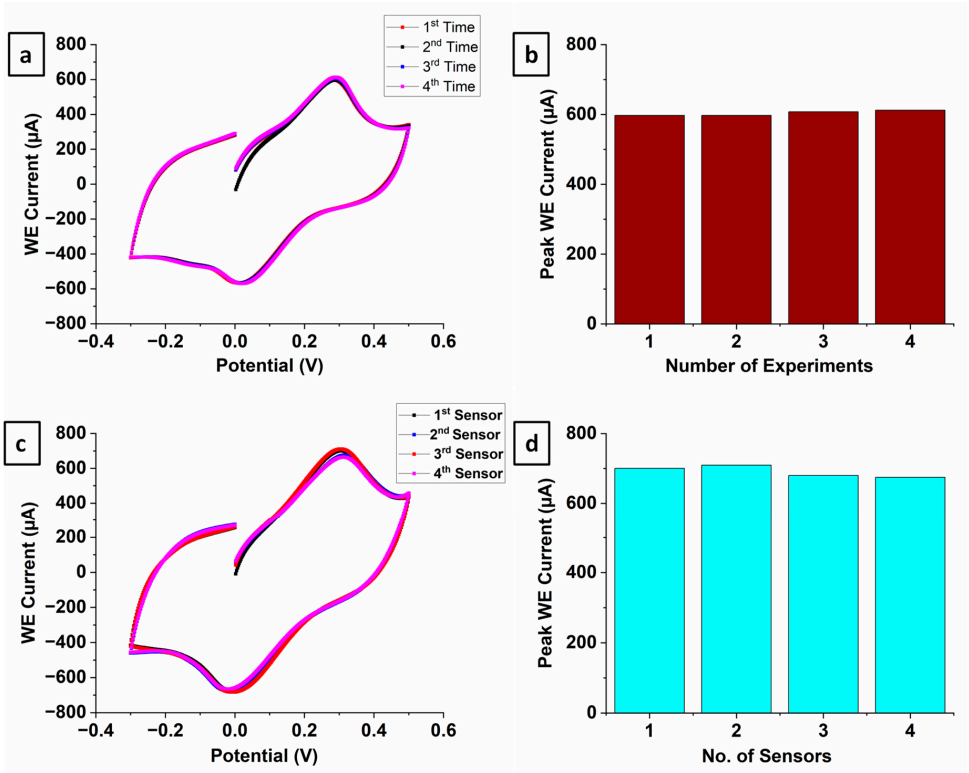


**Figure 6.** (**a**) CV responses of 200 nM of dopamine in 0.1 M PBS (pH 7.4) with $Fe^{2+}/Fe^{3+}$ redox probes when applied to same electrode. (**b**) Corresponding histogram showing the peak W.E. current variation with respect to number of experiments. (**c**) CV responses of 100 nM of dopamine in 0.1 M PBS (pH 7.4) with $Fe^{2+}/Fe^{3+}$ redox probes when applied to four different electrodes. (**d**) Corresponding histogram showing the peak W.E. current variation with respect to different sensors.

Additionally, to assess the reproducibility of the proposed dopamine sensor, four sensors were independently fabricated under identical conditions, and their cyclic voltammetry (CV) responses to 100 nM dopamine were measured, as presented in Figure 6c. The analytical responses were consistent, with a relative standard deviation (RSD) of 2.3% for peak current (Ip) values ($n$ = 4), indicating that the biosensor exhibits high reproducibility. The smallest variability that is found in the reproducibility current may be due to the manual preparation of the sensor.

## 5. Conclusions

In this work, a novel sensor design was developed for rapid and efficient dopamine detection, offering enhanced performance due to its increased working area compared to commercially available sensors. SEM, XRD, and FTIR analyses confirmed the successful formation of laser-induced graphene in the presence of G-PANI ink. The sensor demonstrated a strong linear correlation between dopamine oxidation peak currents and concentrations ranging from 0.1 μM to 100 μM, while those examined by cyclic voltammetry and Chronoamperometry had an LOD of 0.043 μM in PBS. The result validated the better performance of this method compared to our fabricated sensor without the interdigitated gear-shaped electrode [24]. This indicates that the improved biosensor could be promising for the early detection of serious diseases, i.e., Parkinson's disease. The sensor also demonstrated high selectivity for dopamine in the presence of interfering substances like ascorbic acid (AA) and uric acid (UA), and it performed effectively in human serum, mimicking real-world testing conditions. Consistency in the repeatability and reproducibility tests was observed, though the manual addition of the G-PANI and silver ink leaves room for slight improvements in reproducibility. Future work will focus on making the sensor wearable and more user-friendly to expand its practical applications. By making the device portable and integrating it with smartphones, we can develop a system capable of continuously monitoring dopamine levels, providing a valuable addition to sensor and actuator networks.

**Author Contributions:** Conceptualization, N.I. and A.A.; methodology, A.A.; software, P.P.S. and R.T.; validation, N.I., A.A. and A.H.J.; formal analysis, P.P.S.; investigation, A.A.; resources, N.I.; data curation, P.P.S.; writing—original draft preparation, P.P.S. and. R.T.; writing—review and editing, A.A., N.I. and A.H.J.; visualization, P.P.S. and R.T.; supervision, N.I.; project administration, N.I.; funding acquisition, N.I. and A.A. All authors have read and agreed to the published version of the manuscript.

**Funding:** This research was funded by the National Science Foundation (NSF) under grant number ERI 2138574, UTRGV Biomedical Engineering Start-up grant, and Bentsen Endowment.

**Institutional Review Board Statement:** Not applicable.

**Data Availability Statement:** The original contributions presented in this study are included in the article; further inquiries can be directed to the corresponding author.

**Acknowledgments:** The authors acknowledge the support provided by Fahmida Alam and G M Mehedi Hossein from the University of Texas Rio Grande Valley.

**Conflicts of Interest:** The authors declare no conflicts of interest.

## References

1. Karim, A.; Yasser, M.; Ahmad, A.; Natsir, H.; Wahid Wahab, A.; Fauziah, S.; Taba, P.; Pratama, I.; Rosalin; Rajab, A.; et al. A review: Progress and trend advantage of dopamine electrochemical sensor. *J. Electroanal. Chem.* **2024**, *959*, 118157. [CrossRef]
2. Matt, S.M.; Gaskill, P.J. Where is dopamine and how do immune cells see it?: Dopamine-mediated immune cell function in health and disease. *J. Neuroimmune Pharmacol.* **2020**, *15*, 114–164. [CrossRef]
3. Steckl, A.J.; Ray, P. Stress Biomarkers in Biological Fluids and Their Point-of-Use Detection. *ACS Sens.* **2018**, *3*, 2025–2044. [CrossRef] [PubMed]
4. Ahmad, K.; Kim, H. Design and fabrication of WO3/SPE for dopamine sensing application. *Mater. Chem. Phys.* **2022**, *287*, 126298. [CrossRef]

5. Rahman, M.A.; Pal, R.K.; Islam, N.; Freeman, R.; Berthiaume, F.; Mazzeo, A.; Ashraf, A. A Facile Graphene Conductive Polymer Paper Based Biosensor for Dopamine, TNF-α, and IL-6 Detection. *Sensors* **2023**, *23*, 8115. [CrossRef]
6. Hou, S.; Kasner, M.L.; Su, S.; Patel, K.; Cuellari, R. Highly Sensitive and Selective Dopamine Biosensor Fabricated with Silanized Graphene. *J. Phys. Chem. C* **2010**, *114*, 14915–14921. [CrossRef]
7. Alam, F.; Jalal, A.H.; Pala, N. Selective Detection of Alcohol Through Ethyl-Glucuronide Immunosensor Based on 2D Zinc Oxide Nanostructures. *IEEE Sens. J.* **2019**, *19*, 3984–3992. [CrossRef]
8. Hossain, G.M.M.; Jalal, A.H.; Pala, N.; Alam, F. Advancements in Glucose Monitoring: A Thin Film ZnO-Nanoflakes Based Highly Sensitive Wearable Biosensor for Noninvasive Sweat-Based Point-of-Care Monitoring for Diabetes. *ECS Trans.* **2024**, *113*, 35–42. [CrossRef]
9. Tabassum, R.; Sarkar, P.P.; Jalal, A.H.; Ashraf, A.; Islam, N. Laser-Induced Electrochemical Biosensor Modified with Graphene-Based Ink for Label-Free Detection of Alpha-Fetoprotein and 17β-Estradiol. *Polymers* **2024**, *16*, 2069. [CrossRef]
10. Singh, A.; Kaushik, A.; Kumar, R.; Nair, M.; Bhansali, S. Electrochemical Sensing of Cortisol: A Recent Update. *Appl. Biochem. Biotechnol.* **2014**, *174*, 1115–1126. [CrossRef]
11. Chung, S.; Akhtar, M.H.; Benboudiaf, A.; Park, D.; Shim, Y. A Sensor for Serotonin and Dopamine Detection in Cancer Cells Line Based on the Conducting Polymer−Pd Complex Composite. *Electroanalysis* **2020**, *32*, 520–527. [CrossRef]
12. Du, Y.; Dai, L.; Yang, F.; Zhang, Y.; An, C. In situ polymerization confinement synthesis of ultrasmall $MoTe_2$ nanoparticles for the electrochemical detection of dopamine. *Inorg. Chem. Front.* **2022**, *9*, 4121–4126. [CrossRef]
13. Arumugasamy, S.K.; Govindaraju, S.; Yun, K. Electrochemical sensor for detecting dopamine using graphene quantum dots incorporated with multiwall carbon nanotubes. *Appl. Surf. Sci.* **2020**, *508*, 145294. [CrossRef]
14. Ghosh, D.; Rahman, M.A.; Ashraf, A.; Islam, N. Graphene-Conductive Polymer-Based Electrochemical Sensor for Dopamine Detection. In Proceedings of the ASME 2022 International Mechanical Engineering Congress and Exposition. Volume 9: Mechanics of Solids, Structures, and Fluids; Micro- and Nano-Systems Engineering and Packaging; Safety Engineering, Risk, and Reliability Analysis; Research Posters, Columbus, OH, USA, 30 October–3 November 2022; p. V009T13A014.
15. Fiore, L.; Mazzaracchio, V.; Serani, A.; Fabiani, G.; Fabiani, L.; Volpe, G.; Moscone, D.; Bianco, G.M.; Occhiuzzi, C.; Marrocco, G.; et al. Microfluidic paper-based wearable electrochemical biosensor for reliable cortisol detection in sweat. *Sens. Actuators B Chem.* **2023**, *379*, 133258. [CrossRef]
16. Lin, J.; Peng, Z.; Liu, Y.; Ruiz-Zepeda, F.; Ye, R.; Samuel, E.L.G.; Yacaman, M.J.; Yakobson, B.I.; Tour, J.M. Laser-induced porous graphene films from commercial polymers. *Nat. Commun.* **2014**, *5*, 5714. [CrossRef]
17. Rahman, H.A.; Rafi, M.; Putra, B.R.; Wahyuni, W.T. Electrochemical Sensors Based on a Composite of Electrochemically Reduced Graphene Oxide and PEDOT:PSS for Hydrazine Detection. *ACS Omega* **2023**, *8*, 3258–3269. [CrossRef]
18. Dzulkurnain, N.A.; Mokhtar, M.; Rashid, J.I.A.; Knight, V.F.; Wan Yunus, W.M.Z.; Ong, K.K.; Mohd Kasim, N.A.; Mohd Noor, S.A. A Review on Impedimetric and Voltammetric Analysis Based on Polypyrrole Conducting Polymers for Electrochemical Sensing Applications. *Polymers* **2021**, *13*, 2728. [CrossRef]
19. Ghosh, D. Graphene-Conductive Ink Coated Laser Engraved Kapton Electrochemical Biosensor for the Detection of Dopamine And Immune-Sensing. Master's Thesis, The University of Texas Rio Grande Valley, Edinburg, TX, USA, 2023.
20. Tabassum, R. Label-Free Laser-Induced Graphene-Based Electrochemical Biosensor Modified with Graphene-Conductive Polymer Ink Coating for Detection of Alpha-Fetoprotein and 17β–Estradiol. Master's Thesis, The University of Texas Rio Grande Valley, Edinburg, TX, USA, 2024. Available online: https://www.proquest.com/docview/3115398615?fromopenview=true&pq-origsite=gscholar&sourcetype=Dissertations%20&%20Theses (accessed on 27 October 2024).
21. Zhu, G.; Ge, Y.; Dai, Y.; Shang, X.; Yang, J.; Liu, J. Size-tunable polyaniline nanotube-modified electrode for simultaneous determination of Pb(II) and Cd(II). *Electrochim. Acta* **2018**, *268*, 202–210. [CrossRef]
22. Zhao, Y.; Yang, X.; Pan, P.; Liu, J.; Yang, Z.; Wei, J.; Xu, W.; Bao, Q.; Zhang, H.; Liao, Z. All-Printed Flexible Electrochemical Sensor Based on Polyaniline Electronic Ink for Copper (II), Lead (II) and Mercury (II) Ion Determination. *J. Electron. Mater.* **2020**, *49*, 6695–6705. [CrossRef]
23. Minta, D.; González, Z.; Melendi-Espina, S.; Gryglewicz, G. Highly efficient and stable PANI/TRGO nanocomposites as active materials for electrochemical detection of dopamine. *Surf. Interfaces* **2022**, *28*, 101606. [CrossRef]
24. Ghosh, D.; Tabassum, R.; Sarkar, P.P.; Rahman, M.A.; Jalal, A.H.; Islam, N.; Ashraf, A. Graphene Nanocomposite Ink Coated Laser Transformed Flexible Electrodes for Selective Dopamine Detection and Immunosensing. *ACS Appl. Bio Mater.* **2024**, *7*, 3143–3153. [CrossRef] [PubMed]
25. Baytemir, G. A non-enzymatic electrochemical sensor based on polyaniline/borophene nanocomposites for dopamine detection. *Appl. Phys. A* **2023**, *129*, 85. [CrossRef]
26. Mahalakshmi, S.; Sridevi, V. In Situ Electrodeposited Gold Nanoparticles on Polyaniline-Modified Electrode Surface for the Detection of Dopamine in Presence of Ascorbic Acid and Uric Acid. *Electrocatalysis* **2021**, *12*, 415–435. [CrossRef]
27. Dokur, E.; Uruc, S.; Kurteli, R.; Gorduk, O.; Sahin, Y. Designing disposable hand-made screen-printed electrode using conductive ink for electrochemical determination of dopamine. *Ionics* **2023**, *29*, 5465–5480. [CrossRef]
28. Suriya Devi, B.; Karthikeyan, R.; Anitha, M.; Prakash, S. Electrochemical incorporation of PVA-ZnO composite on Screen printed carbon electrode as dopamine sensor. *Surf. Interfaces* **2024**, *52*, 104882. [CrossRef]

29. Sakthivel, P.; Ramachandran, K.; Maheshvaran, K.; Senthil, T.S.; Manivel, P. Simultaneous electrochemical detection of ascorbic acid, dopamine and uric acid using Au decorated carbon nanofibers modified screen printed electrode. *Carbon Lett.* **2024**, *34*, 2325–2341. [CrossRef]
30. Yang, F.; Han, X.; Ai, Y.; Shao, B.; Ding, W.; Tang, K.; Sun, W. A Portable Electrochemical Dopamine Detector Using a Fish Scale-Derived Graphitized Carbon-Modified Screen-Printed Carbon Electrode. *Molecules* **2024**, *29*, 744. [CrossRef]
31. Hussaini, A.A.; Sarilmaz, A.; Ozel, F.; Erdal, M.O.; Yıldırım, M. $CeO_2$:$BaMoO_4$ nanocomposite based 3D-printed electrodes for electrochemical detection of the dopamine. *Mater. Sci. Semicond. Process.* **2024**, *180*, 108587. [CrossRef]
32. Arbabi, N.; Beitollahi, H. $Ti_3C_2$ Nano Layer Modified Screen Printed Electrode as a Highly Sensitive Electrochemical Sensor for the Simultaneous Determination of Dopamine and Tyrosine. *Surf. Eng. Appl. Electrochem.* **2022**, *58*, 13–19. [CrossRef]
33. Chen, C.; Ren, J.; Zhao, P.; Zhang, J.; Hu, Y.; Fei, J. A novel dopamine electrochemical sensor based on a β-cyclodextrin/Ni-MOF/glassy carbon electrode. *Microchem. J.* **2023**, *194*, 109328. [CrossRef]
34. Zhang, L.; Tang, J.; Li, J.; Li, Y.; Yang, P.; Zhao, P.; Fei, J.; Xie, Y. A novel dopamine electrochemical sensor based on 3D flake nickel oxide/cobalt oxide @ porous carbon nanosheets/carbon nanotubes/electrochemical reduced of graphene oxide composites modified glassy carbon electrode. *Colloids Surf. Physicochem. Eng. Asp.* **2023**, *666*, 131284. [CrossRef]
35. García-Miranda Ferrari, A.; Foster, C.W.; Kelly, P.J.; Brownson, D.A.; Banks, C.E. Determination of the electrochemical area of screen-printed electrochemical sensing platforms. *Biosensors* **2018**, *8*, 53. [CrossRef] [PubMed]
36. Rag S, A.; Selvakumar, M.; De, S.; Chidangil, S.; Bhat, S. Laser induced graphene with biopolymer electrolyte for supercapacitor applications. *Mater. Today Proc.* **2022**, *48*, 365–370. [CrossRef]
37. Bandgar, D.K.; Khuspe, G.D.; Pawar, R.C.; Lee, C.S.; Patil, V.B. Facile and novel route for preparation of nanostructured polyaniline (PANi) thin films. *Appl. Nanosci.* **2014**, *4*, 27–36. [CrossRef]
38. Nayak, R.; Shetty, P.; Selvakumar, M.; Rao, A.; Rao, K.M. Formulation of new screen printable PANI and PANI/Graphite based inks: Printing and characterization of flexible thermoelectric generators. *Energy* **2022**, *238*, 121680. [CrossRef]
39. Navarchian, A.H.; Joulazadeh, M.; Karimi, F. Investigation of corrosion protection performance of epoxy coatings modified by polyaniline/clay nanocomposites on steel surfaces. *Prog. Org. Coat.* **2014**, *77*, 347–353. [CrossRef]
40. Elgrishi, N.; Rountree, K.J.; McCarthy, B.D.; Rountree, E.S.; Eisenhart, T.T.; Dempsey, J.L. A Practical Beginner's Guide to Cyclic Voltammetry. *J. Chem. Educ.* **2018**, *95*, 197–206. [CrossRef]
41. Leslie, N.; Mauzeroll, J. Spatially resolved electrochemical measurements. In *Encyclopedia of Solid-Liquid Interfaces*; Elsevier: Amsterdam, The Netherlands, 2024; pp. 461–478. [CrossRef]
42. Balkourani, G.; Brouzgou, A.; Tsiakaras, P. A review on recent advancements in electrochemical detection of dopamine using carbonaceous nanomaterials. *Carbon* **2023**, *213*, 118281. [CrossRef]
43. Liu, G.; Iyengar, S.G.; Gooding, J.J. An Electrochemical Impedance Immunosensor Based on Gold Nanoparticle-Modified Electrodes for the Detection of HbA1c in Human Blood. *Electroanalysis* **2012**, *24*, 1509–1516. [CrossRef]
44. Hayashi, Y.; Matsuda, R.; Ito, K.; Nishimura, W.; Imai, K.; Maeda, M. Detection Limit Estimated from Slope of Calibration Curve: An Application to Competitive ELISA. *Anal. Sci.* **2005**, *21*, 167–169. [CrossRef]
45. Bhalla, N.; Jolly, P.; Formisano, N.; Estrela, P. Introduction to biosensors. *Essays Biochem.* **2016**, *60*, 1–8. [CrossRef] [PubMed]
46. Ping, J.; Wu, J.; Wang, Y.; Ying, Y. Simultaneous determination of ascorbic acid, dopamine and uric acid using high-performance screen-printed graphene electrode. *Biosens. Bioelectron.* **2012**, *34*, 70–76. [CrossRef] [PubMed]